Effect of a thin floating fluid layer in parametrically forced waves

ELENA B. MARTÍN
Universidad de Vigo
Área de Mecánica de Fluidos
9 Campus Lagoas-Marcosende, 36310 Vigo
SPAIN
emortega@uvigo.es

JOSE M. VEGA
Universidad Politécnica de Madrid
E. T. S. Ingenieros Aeronáuticos
3 Plaza Cardenal Cisneros, 28040 Madrid
SPAIN

Abstract: In order to describe correctly on-board experiments, where residual acceleration can have a significant impact in the fluid motion, we consider the effect of a thin immiscible fluid layer on top of a liquid substrate in incrementing the damping and promoting drift instabilities in spatially uniform standing Faraday waves. It is seen that the effective surface viscosity of the newtonian liquid film enhances drift instabilities that lead to various steadily travelling and standing and travelling oscillatory patterns, among others. In particular, travelling waves appear to be the primary instability of the basic standing wave for deep water problems.

Key–Words: Faraday instability, weakly nonlinear analysis, oscillatory boundary layers, streaming flow, immiscible liquid film, surface viscosity, on-board experiments, vertically vibrated container.

1 Introduction

In this paper we examine the effect of vertical vibration on an opened-container filled with liquid in presence of a controlled surface contamination. The motivation is to describe correctly on-board experiments where residual acceleration, due to crew manoeuvring and machinery, can have a significant impact in the fluid motion. In general, residual oscillatory acceleration, or g-jitter, is broad-band and varies randomly both in magnitude and direction. This acceleration is usually transmitted through the container walls of the fluid system. Thus the actual excitation of the fluid is transmitted via the narrow-band structural response centered on the natural frequencies of the support structure. Although the random nature of the vibration cannot be ignored, the usual first step is to take the vibration as monochromatic, with a constant amplitude and direction in order to obtain physical insight into the fundamental mechanisms. The surface waves that appear (also known as Faraday waves [1]) when the forcing amplitude exceeds a threshold value have attracted a great deal of attention because of the rich variety of non-linear pattern forming phenomena that the Faraday instability exhibits (see [2] and references therein). The correct nonlinear amplitude equations used to described this weakly nonlinear regime ([3],[4],[5]) take into account the presence of the slow non oscillatory mean flow that is driven by the boundary layers at the container walls and free surface and, in the case of a monochromatic wave ([6] and [7]) predicts periodic standing waves (PSW) and constant velocity travelling waves (TW) after onset that have been observed experimentally in annular containers ([8], [9]) and in semitoroidal water rings ([10]). The presence of surface contamination or controlled surfactants at the free surface is critical for determining not only the critical amplitude above which the standing waves appear ([11],[12],[13]), but also the behavior of the Faraday waves after onset, as seen in [7]. All these free surface alterations change completely the structure of the oscillating upper boundary layer attached at the free surface and, in consequence, the forcing mechanisms of the mean flow. In this paper we analyze the effect of a thin floating fluid layer on top of a liquid substrate, modelled with surface shear and dilatational viscosity based on the Boussinesq-Scriven surface model ([14], [15] and [7] for details), in incrementing the damping and promoting drift instabilities in spatially uniform standing Faraday waves. This paper is organized as follows: in §2 we shall present the systems of equations for the slow time evolution of the surface waves and the mean flow, derived from the full Navier-Stokes equations that described the problem assuming that the fluid layer is thick enough to behave like a Newtonian fluid, yet thin enough for the variation of the velocity field within the film to be reasonably small. In this

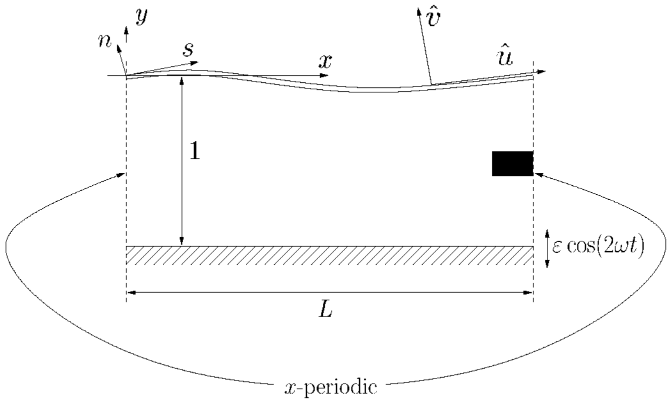

Figure 1: Sketch of the dimensionless fluid domain.

case the effective surface viscosity is proportional to $\mu_f h_f$, where μ_f is the volumetric viscosity of the liquid film and h_f is the film thickness ([16]); the relevant large-time patterns resulting from the primary bifurcations will be described in §3 and finally the main conclusions will be summarize in §4.

2 Coupled Amplitude-Mean Flow Equations

We consider a horizontal 2-D liquid (of density ρ and viscosity μ) supported by a vertically vibrating plate. On top of the liquid there is a floating inmiscible fluid film of volumetric viscosity μ_f and thickness h_f. Using the container's depth h and the gravitational time $\sqrt{h/g}$ for nondimensionalization (figure 1), we obtain the following governing equations

$$u_x + v_y = 0, \tag{1}$$

$$u_t + v(u_y - v_x) = -q_x + C(u_{xx} + u_{yy}), \tag{2}$$

$$v_t - u(u_y - v_x) = -q_y + C(v_{xx} + v_{yy}), \tag{3}$$

$$u = v = 0 \quad \text{at} \quad y = -1, \tag{4}$$

$$\begin{gathered} v = f_t + u f_x, \quad C^{1/2}(\hat{u}_n + \hat{v}_s + \kappa\hat{u}) = \delta\hat{u}_{ss}, \\ q - \frac{u^2+v^2}{2} + 4\omega^2\varepsilon f\cos(2\omega t) - f + T\kappa = \\ = 2C\hat{v}_n \quad \text{at } y = f, \end{gathered} \tag{5}$$

$$u,\ v,\ q \text{ and } f \text{ are } L\text{-periodic in } x, \tag{6}$$

where

$$s = \int_0^x \sqrt{1+f_x^2}\, dx \quad \text{and} \quad \kappa = \frac{f_{xx}}{(1+f_x^2)^{3/2}} \tag{7}$$

are an arch length parameter and the curvature of the free surface (defined as $y = f$), respectively, and n is a coordinate along the upward unit normal to the free surface; $\hat{u}$ and $\hat{v}$ are the tangential and normal velocity components at the free surface $y = f$, which are related to the horizontal and vertical components u and v by

$$\hat{u} = \frac{u + f_x v}{\sqrt{1+f_x^2}}, \quad \hat{v} = \frac{v - f_x u}{\sqrt{1+f_x^2}}. \tag{8}$$

Equations (1)-(6) formulate the problem when dealing with a floating fluid layer on top of the liquid. The only difference between these equations and the formulation of the problem for a clean surface is the boundary condition (5b), whose right hand side is equal to zero for the clean surface and now accounts for the presence of the fluid film, modelled in the simplest way, where the resulting tangential stress includes the surface viscosity effects. Scriven [15] generalized the mathematical description of the Boussinesq [14] treatment for a time-dependent interface for which the interfacial stress is a linear function of two intrinsic properties of the interface, namely the surface shear viscosity μ_1^S and the surface dilatational viscosity μ_2^S, both assumed constants here. The (two dimensional) surface stress is written as $\boldsymbol{\tau} = \boldsymbol{\nabla}_S T^* + (\mu_2^S - \mu_1^S)\boldsymbol{\nabla}_S(\boldsymbol{\nabla}_S \cdot \boldsymbol{v}^S) + \mu_1^S \boldsymbol{\nabla}_S \cdot [\boldsymbol{\nabla}_S \boldsymbol{v}^S + (\boldsymbol{\nabla}_S \boldsymbol{v}^S)^\top]$, where $\boldsymbol{\nabla}_S$ is the (two dimensional) surface gradient operator, $\boldsymbol{v}^S$ is the (two dimensional) surface velocity vector, and $\top$ denotes the transpose. The boundary condition (5b) results from equating the surface stress to the viscous shear stress from the bulk at the free surface, and nondimensionalizing. It follows that the nondimensional surface viscosity is given by $\delta = (\mu_1^S + \mu_2^S)/(\mu h)\sqrt{C}$, with C defined below.

For very thin films or monolayers of thickness up to 100-1000 times the length of the molecules of the film (500-1000 nm) the surface viscosities μ_1^S and μ_2^S do not seem to be simply related to the volumetric viscosity of the fluid in contrast with the case of a film thick enough to behave like a Newtonian fluid and sufficiently thin for the variation of the velocity within the film to be reasonably small. In this case, assuming that the thickness of the fluid layer is less than the thickness of the oscillating boundary layer that can be created in the film, the (two-dimensional) surface shear viscosity can be expressed as $\mu_f h_f$ and the (two-dimensional) surface dilatational viscosity as $3\mu_f h_f$ ([16]). Since the wave-induced tangential surface motions are essentially one-dimensional, the surface shear and dilatational surface viscosities are added giving the following effective surface viscosity number

$$\delta = \frac{4\mu_f h_f}{\mu h}\sqrt{C} \tag{9}$$

The dimensionless problem (1)-(6) depends on the following nondimensional parameters: the forcing frequency $2\omega = 2\omega^*\sqrt{h/g}$ and amplitude $\varepsilon = \varepsilon^*/h$, the ratio of viscous to gravitational effects $C = \mu/(\rho\sqrt{gh^3})$, the Bond number $T^{-1} = \rho g h^2/T^*$ (T^* = surface tension), the horizontal aspect ratio $L = L^*/h$ (L^* = horizontal length of the domain) and the effective surface viscosity number δ.

We shall consider small, nearly-resonant solutions at small viscosity, i.e.,

$$\begin{aligned} &|u| + |v| + |q| + |f| \ll 1, \quad \varepsilon \ll 1, \\ &|\omega - \omega_0| \ll 1, \quad C \ll 1. \end{aligned} \tag{10}$$

The assumption that $C \ll 1$ is reasonable for not too viscous fluids in not too thin layers. Frequency ω_0 in (10) is a natural frequency in the inviscid limit ($C = 0$).

The effective surface viscosity number δ can vary in a wide range depending on the nature and the thickness of the fluid film and substrate ([16], [17]). As an example, the surface viscosity number for a container depth of $h = 10$ cm filled with water ($C = 10^{-5}$) and a film of silicone oil (Dow Corning 200 Fluid, $\nu_f = 6 \times 10^{-2}\text{m}^2/\text{s}$, $\rho_f = 969$ kg/m^3) of thickness $h_f = 5$ mm is $\delta = 36.77$, while for a 1 mm depth of SAE-30 oil film ($\nu_f = 5.5 \times 10^{-4}\text{m}^2/\text{s}$, $\rho_f = 727$ kg/m^3 at 20 C) and the same liquid substrate the effective surface viscosity number is $\delta = 0.05$. Note that the film dimensionless thickness must obey the following relationship

$$\frac{h_f}{h} \ll \sqrt{C}\left(\frac{\nu_f}{\nu}\right)^{1/2} \ll 1, \tag{11}$$

where ν_f and ν are the kinematic viscosities of the film and substrate respectively, to ensure the thickness of the fluid layer is smaller than the oscillating film boundary layer. Thus, in the rest of this work we will not make any assumption on the value of the effective surface viscosity number δ.

As explained in [6] and [18], the solution can be expanded as an oscillating first part caused by the oscillatory inviscid modes (with a $\mathcal{O}(1)$ frequency and a $\mathcal{O}(\sqrt{C})$ decay rate) and a slow non-oscillatory secondary part generated by the viscous modes (with a $\mathcal{O}(C)$ decay rate), that produce the mean flow. The solution in the bulk region, outside the boundary layers that appear at the free surface and the bottom plate, is written as follows

$$\begin{aligned} u &= U_0(y)e^{i\omega t}[A(t)e^{ikx} - B(t)e^{-ikx}] + c.c.+ \\ &\quad + u^m(x,y,t) + \cdots, \\ v &= iV_0(y)e^{i\omega t}[A(t)e^{ikx} + B(t)e^{-ikx}] + c.c.+ \\ &\quad + v^m(x,y,t) + \cdots, \\ q &= Q_0(y)e^{i\omega t}[A(t)e^{ikx} + B(t)e^{-ikx}] + c.c.+ \\ &\quad + q^m(x,y,t) + \cdots, \\ f &= e^{i\omega t}[A(t)e^{ikx} + B(t)e^{-ikx}] + c.c.+ \\ &\quad + f^m(x,t) + \cdots, \end{aligned} \tag{12}$$

where $c.c$ stands for the complex conjugate, $k = 2m\pi/L$ (with m a positive integer) is the horizontal wave number and U_0, V_0 and Q_0 are the corresponding inviscid eigenfunctions

$$U_0 = -\frac{kQ_0}{\omega_0},\ V_0 = \frac{Q_{0y}}{\omega_0},\ Q_0 = \frac{\omega_0^2 \cosh k(y+1)}{k \sinh k}, \tag{13}$$

$$\omega_0^2 = k(1 + Tk^2)\tanh k. \tag{14}$$

The terms displayed above correspond to the only surface mode that is sub-harmonically excited by the external forcing and the mean flow, that will be denoted hereinafter by the superscript m. Dependence of the complex amplitudes A and B on x is ignored for simplicity. The weakly nonlinear analysis requires the amplitudes A and B to be small and depend slowly on time $|A'| \ll |A| \ll 1$, $|B'| \ll |B| \ll 1$

If we insert expansions (12) into the governing equations, take into account the boundary layers at the free surface and the bottom of the container and apply solvability conditions, the following equations for the evolution of the complex amplitudes are obtained

$$\begin{aligned} A' &= [-d_1 - id_2 + \mathrm{i}\alpha_3|A|^2 - \mathrm{i}\alpha_4|B|^2 - \\ &\quad - \mathrm{i}\frac{\alpha_6}{L}\int_{-1}^{0}\int_0^L g(y)u^m dx dy]A + \mathrm{i}\varepsilon\alpha_5\bar{B}, \end{aligned} \tag{15}$$

$$\begin{aligned} B' &= [-d_1 - id_2 + \mathrm{i}\alpha_3|B|^2 - \mathrm{i}\alpha_4|A|^2 + \\ &\quad + \mathrm{i}\frac{\alpha_6}{L}\int_{-1}^{0}\int_0^L g(y)u^m dx dy]B + \mathrm{i}\varepsilon\alpha_5\bar{A}, \end{aligned} \tag{16}$$

and depend on the mean flow through a non local term. See [6] for a more detailed derivation of similar amplitude equations without the presence of a film layer. The expressions of the coefficients and the function $g(y)$ coincide with their counterparts in [6] and [7] except for d_1 and d_2 that now accounts for the effective surface viscosity of the fluid film

$$d_1 = \alpha_1 C^{1/2}, \quad d_2 = \alpha_2 C^{1/2} + \omega_0 - \omega, \tag{17}$$

$$\begin{aligned} \alpha_1 + \mathrm{i}\alpha_2 = & \frac{k\sqrt{i\omega_0}}{\sinh 2k} + \\ & + \frac{\delta\sqrt{i\omega_0}\omega_0 k^3}{2\tanh k[\omega_0\sqrt{i\omega_0} + \delta\omega_0 k^2]}. \end{aligned} \tag{18}$$

The damping of the Faraday waves is clearly increased by the presence of the floating film, specially for deep water problems, as can be seen by comparison with the damping for a clean free surface problem ([18]) that becomes of the order of C for moderately large values of the surface wave number k.

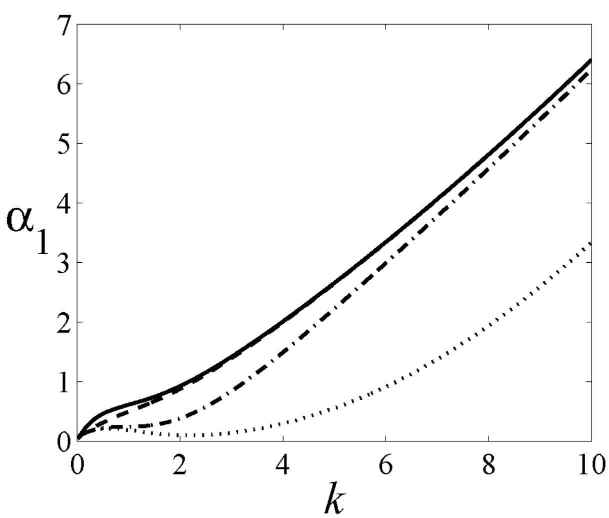

Figure 2: The damping ratio α_1 in terms of k for gravity waves with $T = 7.42 \cdot 10^{-4}$ and: (——) $\delta = 10$, (— — —) $\delta = 1$, (— · — · —) $\delta = 0.1$, and (· · · · ·) $\delta = 0.01$.

After a transient, the solution of equations (15) and (16) always relaxes to a standing wave ($|A| = |B| = R_0$) of the form

$$f(x,t) = 4R_0 \cos(\omega t + \phi_0)\cos[k(x-\psi)] \tag{19}$$

with constant amplitude R_0 (which depends on the amplitude of the applied forcing) and spatial phase $\psi(t)$ that remains coupled to the streaming flow through the equation (20b)

$$\begin{aligned} R_0^2 &= \frac{d_2 \pm (\alpha_5^2\varepsilon^2 - d_1^2)^{1/2}}{\alpha_3 - \alpha_4}, \\ \psi' &= \frac{\alpha_6}{kL}\int_{-1}^{0}\int_0^L g(y)u^m dx dy. \end{aligned} \tag{20}$$

Ignoring the initial transient, taking into account the last result in expansions (12a)-(12d) and introducing these expressions into (1)-(6), we obtain the following equations for the mean flow outside the two boundary layers

$$\tilde{u}_x + \tilde{v}_y = 0, \tag{21}$$

$$\frac{\partial \tilde{u}}{\partial \tau} + \tilde{v}(\tilde{u}_y - \tilde{v}_x) = -\tilde{q}_x + Re^{-1}(\tilde{u}_{xx} + \tilde{u}_{yy}), \tag{22}$$

$$\frac{\partial \tilde{v}}{\partial \tau} - \tilde{u}(\tilde{u}_y - \tilde{v}_x) = -\tilde{q}_y + Re^{-1}(\tilde{v}_{xx} + \tilde{v}_{yy}), \tag{23}$$

$\tilde{u}, \tilde{v}$ and $\tilde{q}$ are x-periodic, of period $L = 2m\pi/k$, (24)

$$\frac{d\psi}{d\tau} = \frac{1}{L}\int_{-1}^{0}\int_0^L G(y)\tilde{u}(x,y,\tau)dxdy, \qquad G(y) = \frac{2k\cosh 2k(y+1)}{\sinh 2k} \tag{25}$$

$$\tilde{u} = -(1-\Gamma)\sin[2k(x-\psi)], \tilde{v} = 0 \text{ at } y = -1, \tag{26}$$

$$\tilde{u} = -\Gamma\sin[2k(x-\psi)], \tilde{v} = 0, \text{ at } y = 0, \tag{27}$$

where, for convenience, we have rescale time and mean flow variables as

$$\tau = ReCt, \; \tilde{u} = \frac{u^m}{ReC}, \; \tilde{v} = \frac{v^m}{ReC}, \; \tilde{q} = \frac{q^m}{(ReC)^2}, \tag{28}$$

with the effective mean flow Reynolds number defined as follows

$$Re = \frac{2R_0^2}{C}(\alpha_7 + \alpha_8), \tag{29}$$

with

$$\begin{aligned} \alpha_7 &= \frac{3\omega_0 k}{\sinh^2 k}, \\ \alpha_8 &= \frac{\omega_0 k}{\tanh^2 k}\Big(\frac{4i\delta\omega_0 k^2}{\omega_0\sqrt{i\omega_0} + \delta\omega_0 k^2} + \text{c.c.} + \\ &\quad + \frac{3\delta^2\omega_0^2 k^4}{|\omega_0\sqrt{i\omega_0} + \delta\omega_0 k^2|^2}\Big). \end{aligned} \tag{30}$$

Equations (21)-(27) depend on the wavenumber k, the spatial period $L = \frac{2\pi m}{k}$ with $m = 1, 2, \ldots$, the

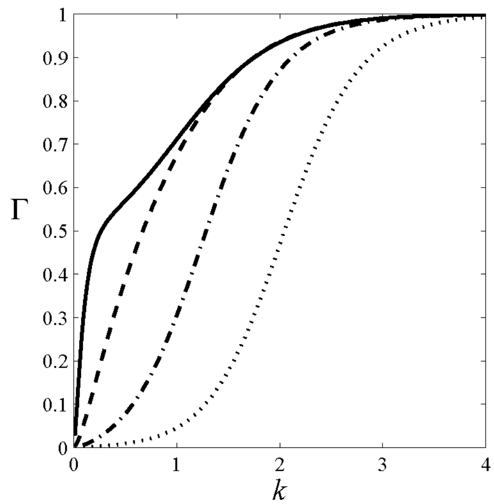

Figure 3: The film parameter Γ vs. k for $T = 7.42 \cdot 10^{-4}$ and: (——) $\delta = 10$, ($- - -$) $\delta = 1$, ($- \cdot - \cdot -$) $\delta = 0.1$, and ($\cdot \cdot \cdot \cdot \cdot$) $\delta = 0.01$.

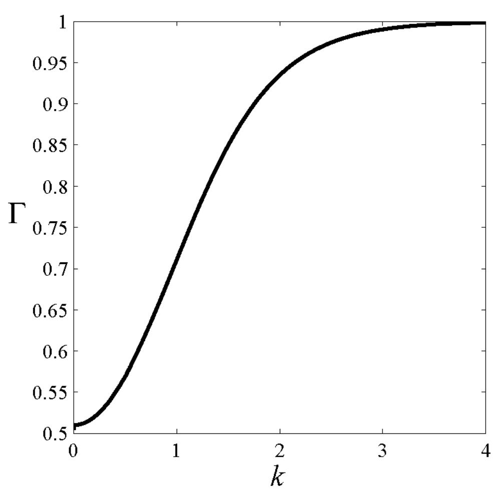

Figure 4: The maximum value of the film parameter Γ vs. k for $T = 7.42 \cdot 10^{-4}$ and varying δ.

effective Reynolds number Re, and the film parameter Γ that measures the relative effect of the surface viscosity of the floating film in the generation of the streaming flow

$$\Gamma = \Gamma(k, T, \delta) \equiv \frac{\alpha_8}{\alpha_7 + \alpha_8}. \qquad (31)$$

The film parameter Γ can vary in the interval [0,1] and is plotted *vs.* the wave number k in figure 3 for the indicated values of δ for $T = 7.42 \cdot 10^{-4}$, that corresponds to the inverse of the Bond number for a 10 cm depth water container. It can be seen that for deep water problems, namely $k > \pi$, the film parameter is of the order of 1, even for quite small values of the effective surface viscosity of the fluid film. Its maximum value is plotted in figure 4 *vs.* k. Note that the presence of the floating layer enhances the strength of the mean flow produced by the surface wave by substituting the upper boundary condition for the mean flow of zero tangential stress (that is, for spatial uniform surface waves with clean free surface should be $\tilde{u}_y = 0$ at $y = 1$) for the $\mathcal{O}(1)$ forcing tangential velocity (27). Detailed deduction of a boundary condition qualitatively similar to (27), that require to solve the upper boundary layer, is explained in [7].

The effective Reynolds number Re is proportional to the wave steepness, $R_0 k$ that should be small. Since C is also small, Re can vary in a wide range. A good estimate for the Reynolds number is

$$0 \le Re \le 2 \times 10^4(\alpha_7 + \alpha_8)/k^2, \qquad (32)$$

which for, e.g. $k = 2.37$ gives $0 \le Re < 5000$ for small values of δ and at least $0 \le Re < 5 \times 10^4$ for values of δ of order 1. We integrate numerically (21)-(27) for some values of the wavenumber k and the spatial period L, varying both the Re and Γ values.

3 Large time patterns

For small values of the effective mean flow Reynolds number Re, the solution relaxes to the basic standing wave (SW) with $\psi' = 0$. The mean flow associated with this basic SW consists of an array of pairs of steady counterrotating eddies that fulfills all the symmetries of equations (21)-(27), that is, it is reflection symmetric in x (thus $\psi' = 0$ and the streaming flow does not affect the surface SW) and $L/2$-symmetric (the solution is repeated twice in the container). Examples of mean flow streamlines for these states (named SW($L/2$)) are plotted in fig.5(a)-5(c) for increasing values of the film parameter. The bigger the film parameter is, the more important the surface eddies are.

This basic state destabilizes through a primary instability that depends on the value of the film parameter. Thus, we chose a value of $k = 2.37$ that mimic a shallow problem because allows as *(i)* to vary Γ in a wide range and *(ii)* to compare with the clean free surface results in [6]. In figure 6(b) it can be seen that

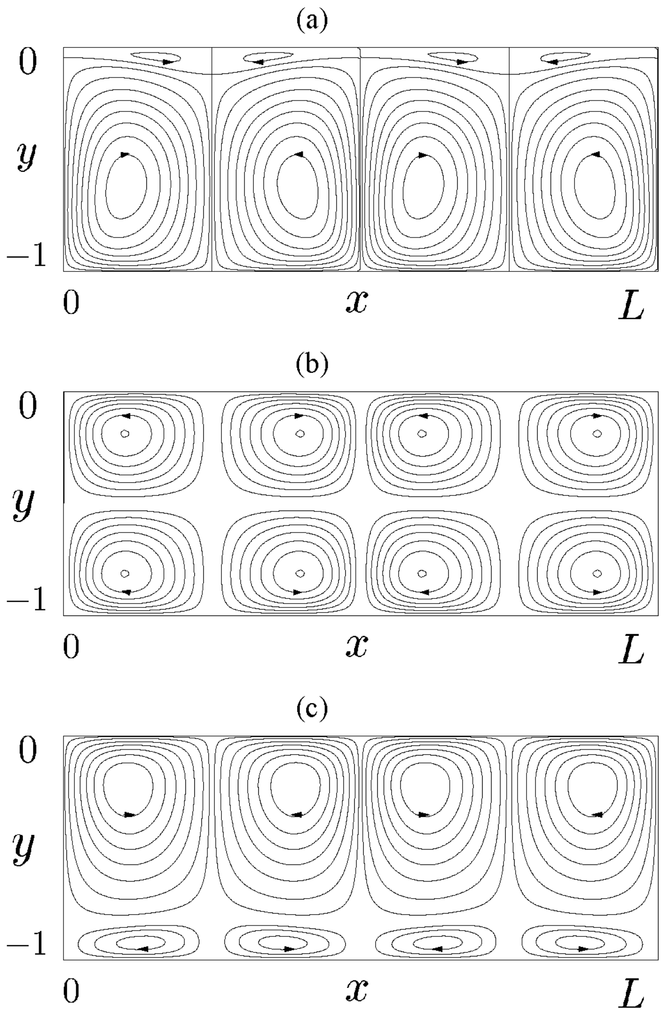

Figure 5: Mean flow streamlines of (21)-(27), for $k = 2.37$, $L = 2.65$ ($m = 1$), and (Re, Γ): (a) $(200, 0.1)$, (b) $(160, 0.5)$, (c) $(60, 0.9)$.

for small values of Γ (approximately $0 < \Gamma < 0.371$) the instability takes place through a Hopf bifurcation and pulsating standing waves (PSW) with no net drift are obtained. Figure 7 shows the mean flow streamlines of a PSW solution as a function of time along the pulsating period of the wave. Note that the mean flow is still $L/2$-symmetric. In order to compare this fluid film case with the clean surface problem ([6]) the critic Reynolds number of destabilization for the clean free surface problem (for the same values of k and L) is marked with a large point in the horizontal axe of figure 6. Thus, for quite small values of the film parameter Γ the film effect seems to stabilize the basic SWs. Secondary bifurcations take place for bigger values of Re that lead, among others, to PSW no longer $L/2$-symmetric, travelling pulsating waves, and chaotic solutions.

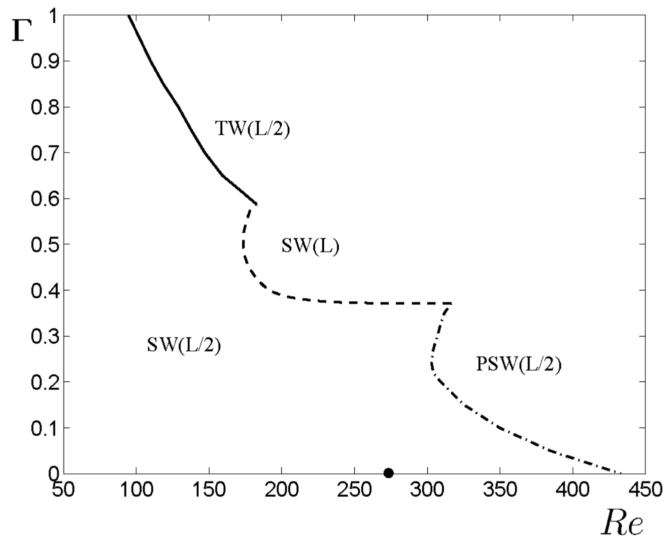

Figure 6: The primary instability of the basic SW for different film parameter values for $k = 2.37$, $L = 2.65m$ (checked for $m = 1, 2, \ldots, 10$). The bifurcation is either a Hopf bifurcation ($- \cdot - \cdot -$) if $0 < \Gamma < 0.371$, a $(L/2)$-symmetry breaking bifurcation ($- - -$) if $0.371 < \Gamma < 0.588$, or a parity breaking bifurcation (——) if $0.588 < \Gamma < 1$.

For an intermediate value of Γ ($0.371 < \Gamma < 0.588$) a symmetry breaking bifurcation to another type of SW no longer $L/2$ symmetric (SW(L)) occurs, see streamlines in figure 8(a) as an example. This type of solution is stable for quite large values of the effective mean flow Reynolds number Re. For larger values of the film parameter (that is, for $0.588 < \Gamma < 1$) the basic SW($L/2$) destabilizes through a parity breaking bifurcation that leads to TWs (TW($L/2$)) whose streamlines for the mean flow in a moving reference frame (that moves with the surface wave velocity) are similar to the one plotted in 8(b). Note that the mean flow is still $L/2$-symmetric. For larger values of the Reynolds number Re, different secondary instabilities are obtained, which include another type of TWs with no $L/2$-symmetric mean flow (figure 5(c)), pulsating travelling waves, more complicated solutions and even chaotic attractors.

We may also note that these three primary instabilities shown in figure 6 for $k = 2.37$ remain unchanged for larger domains (checked for $L = \frac{2\pi m}{k}$ with $m = 1, 2, \ldots, 10$). For different values of the

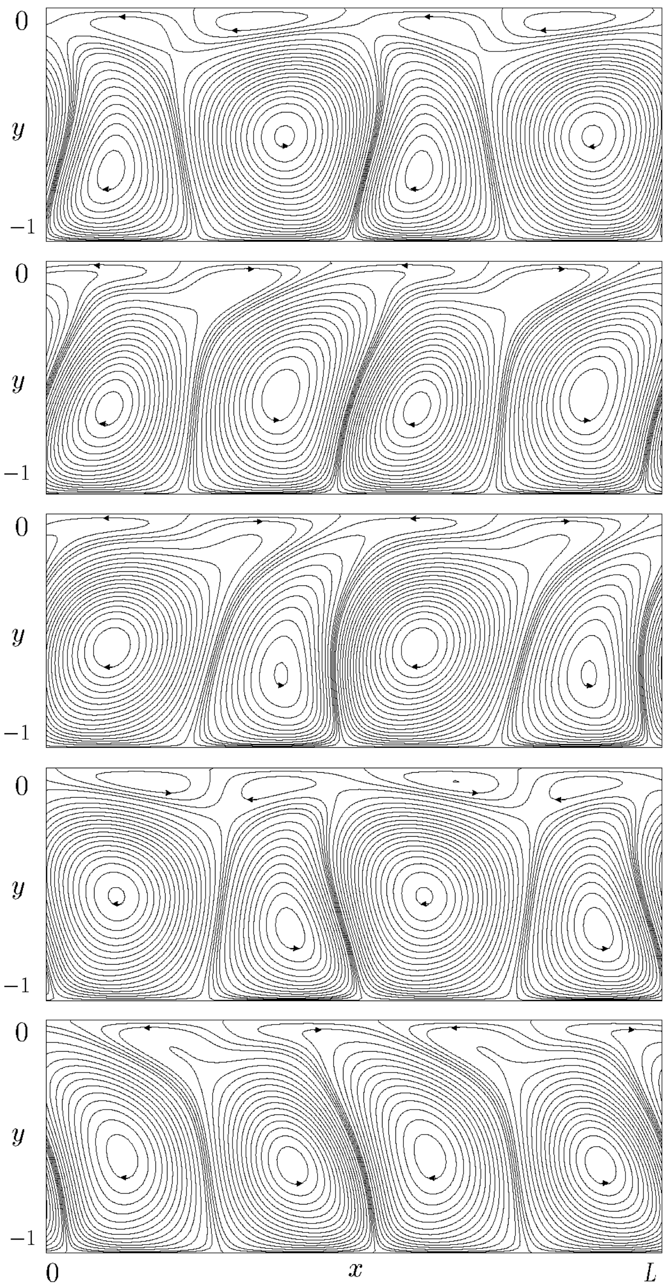

Figure 7: Streamlines of a pulsating standing wave for different values of τ along the period T, ($\tau = \frac{T}{6}, \frac{2T}{6}, \frac{3T}{6}, \frac{4T}{6}, \frac{5T}{6}$) for $k = 2.37$, $L = 2.65$ ($m = 1$), and $(Re, \Gamma) = (400, 0.2)$

wave number k for deep water problems, where $\gamma \simeq 1$, qualitatively similar results are obtained and the primary instability is always through a parity breaking bifurcation from SWs to TWs.

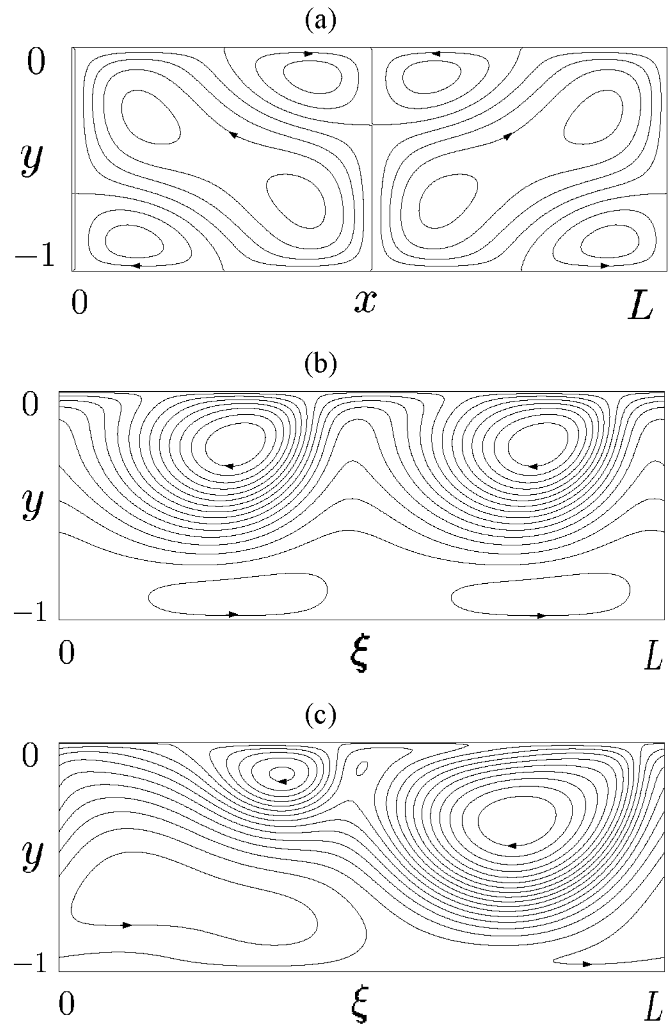

Figure 8: The streamlines for some representative steady (a) and steadily travelling ((b),(c)) attractors of (21)-(27), for $k = 2.37$, $L = 2.65$ ($m = 1$) and the following values of (Re, Γ): (a) $(200, 0.5)$, (b) $(200, 0.9)$, and (c) $(600, 0.9)$. The streamlines of (b) and (c) correspond to moving axes $\xi = x - \psi' \tau$, with the constant drift velocity $\psi' = -0.072$, -0.097, and -0.049, respectively.

4 Conclusions

We analyze the effect of a thin liquid film on top of a liquid substrate that is vertically vibrated with a forcing amplitude sufficiently strong to produce surface waves but weak enough to allow a weakly nonlinear analysis. We assume that the immiscible fluid layer is thick enough to behave as a Newtonian fluid and sufficiently thin for the variation of the velocity within the film to be reasonably small. Thus, the fluid film surface viscosities can be expressed as function of liquid substrate properties and a set of coupled amplitude-mean flow equations that depend on a film parameter named Γ are derived in the nearly inviscid limit.

For shallow water problems, namely $k < \pi$, different states appear depending on the effective surface viscosity number δ. For quite small values of δ, the effective film parameter Γ is moderately small and in this case the primary instability that takes place is a Hopf bifurcation that gives a direct transition from SWs to PSWs. This is also the first instability that occurs in the clean surface case ([6]) (if surface contamination is not present) although for smaller effective Reynolds numbers Re. Thus, the presence of the fluid film (that leads to an small tangential forcing velocity of the mean flow in the upper boundary layer instead of the zero tangential shear stress of the clean surface problem) seems to stabilize the SWs solution. For intermediate values of the film parameter a transition between two steady states for the mean flow is obtained, not affecting the surface wave. This SWs solution is stable for a very wide range of values of Re and this fact might point out to the use of a fluid film as an stabilization mechanism of the surface standing wave by controlling the relative film thickness h_f/h.

For deep water problems, and in contrast with the clean case, a direct primary bifurcation from SWs to TWs appear for nearly all fluid film configurations. This transition is quite robust (remain unchanged for larger domains and appear for all values of the wave number we have checked) and takes place for quite small Re. Thus, the presence of the fluid film destabilizes the surface standing wave.

Therefore, film effects seem to play an important role in the surface waves dynamics. For all these states that are not steady SW, the coupling with the mean flow is an essential ingredient that should not be ignored. For deep water configurations the presence of the fluid film enhances dramatically this coupling between the surface wave and the streaming flow. We expect even more coupling in the three-dimensional annular container as a result of the Stokes boundary layers attached to the lateral walls, which are not present in the two-dimensional model. We encourage further experimental work in the Faraday system in annular containers with a special attention to the streaming flow with and without the presence of a fluid film, in order to achieve a better understanding of the physical mechanisms involved in on-board fluid experiments.

This work was supported by the National Aeronautics and Space Administration (Grant NNC04GA47G) and the Spanish Ministry of Education (Grant MTM2004-03808).

References:

[1] M. Faraday, On the forms and states assumed by fluids in contact with vibrating elastic surfaces. *Phil. Trans. R. Soc. Lond.*, 121, 1831, pp. 319–340.

[2] J. Miles, D. and Henderson On the forms and states assumed by fluids in contact with vibrating elastic surfaces. *Annu. Rev. Fluid Mech.*, 22, 1990, pp. 143–165.

[3] J.M. Vega, E. Knobloch and C. Martel Nearly inviscid Faraday waves in annular containers of moderately large aspect ratio. *Physica D*, 154, 2001, pp. 147–171.

[4] Higuera, M., Vega, J.M. and Knobloch, E. Coupled amplitude-mean flow equations for nearly-inviscid Faraday waves in moderate. *Physica D*, 173, 2002, pp. 178–203.

[5] Mancebo, F. and Vega, J.M.: Viscous Faraday waves in two-dimensional large-aspect-ratio containers. *J. Fluid Mech.*, 560, 2006, pp. 369393..

[6] Martín, E., Martel, C. and Vega, J.M.: Drift instability of standing Faraday waves. *J. Fluid Mech.*, 467, 2002, pp. 57–79.

[7] Martín, E. & Vega, J.M.: The effect of surface contamination on the drift instability of standing Faraday waves. *J. Fluid Mech.*, 546, 2006, pp. 203–225.

[8] Douady, S. Fauve, S. and Thual, O.:, Oscillatory phase modulation of parametrically forced surface waves. *Europhys. Lett.*, 10, 1989, pp. 309–315.

[9] Thual, O., Douady, S. and Fauve, S.:*Instabilities and Nonequilibrium Structures II.* Ed. Tirapegui, E. and Villaroel, D., Kluwer, 227, 1989.

[10] Jung, S., Kim, E. and Shelley, M., J.:*Surface waves in semitoroidal water ring. Phys. Fluids*, 19, 2007.

[11] Kumar S. & Matar O. K.: Parametrically driven surface waves in surfactant-covered liquids. *Proc. R. Soc. Lond. A*, 458, 2002, pp. 2815–2828.

[12] Kumar S., Matar O. K. and Craster, R. V.: Nonlinear waves in vibrated surfactant-covered thin films. *J. Fluid Mech.*, 520, 2004, pp. 243–265.

[13] Ubal S., Giavedoni M. D. & Saita, F.: Elastic effects of an insoluble surfactant on the onset of two-dimensional Faraday waves: a numerical experiment. *J. Fluid Mech.*, 524, 2005, pp. 305–329.

[14] Boussinesq, J. Existence of a superficial viscosity in the thin transition layer separating one liquid from another contiguous fluid. *C. R. Hehbd. Seances Acad. Sci.*,156, 1913, pp. 983–989.

[15] Scriven, L.,E. Dynamics of a fluid interface. *Chem. Eng. Sci.*, 12, 1960, pp. 98–108.

[16] Jenkins, A.D. and Dysthe, K.B.: The effective film viscosity of a thin floating fluid layer. *J. Fluid Mech.*, 344, 1997, pp. 335–337.

[17] Hirsa, A.H., López, J.M. and Miraghaie: Determination of surface shear viscosity via deep-channel flow with inertia. *J. Fluid Mech.*, 470, 2002, pp. 135–149.

[18] Martel C. & Knobloch, E., Damping of nearly-inviscid water waves. *Phys. Rev. E*, 56, 1997, pp. 5544-5548.